Effects of Cytochalasin B on Actin and Myosin Association with Particle Binding Sites in Mouse Macrophages: Implications with Regard to the Mechanism of Action of the Cytochalasins

RICHARD G. PAINTER, JAMES WHISENAND, and ANN T. McINTOSH
Department of Immunopathology, Scripps Clinic and Research Foundation, La Jolla, California 92037

ABSTRACT The intracellular distribution of F-actin and myosin has been examined in mouse peritoneal macrophages by immunofluorescence microscopy. In resting, adherent cells, F-actin was distributed in a fine networklike pattern throughout the cytoplasm. Myosin, in contrast, was distributed in a punctate pattern. After treatment with cytochalasin B (CB), both proteins showed a coarse punctate pattern consistent with a condensation of protein around specific foci. When CB-pretreated cells were exposed to opsonized zymosan particles, immunofluorescent staining for F-actin and myosin showed an increased staining under particle binding sites. Transmission electron microscope (TEM) examination of whole-cell mounts of such preparations revealed a dense zone of filaments beneath the relatively electron-translucent zymosan particles. At sites where particles had detached during processing, these filament-rich areas were more clearly delineated. At such sites dense arrays of filaments that appeared more or less randomly oriented were apparent. The filaments could be decorated with heavy meromyosin, suggesting that they were composed, in part, of F-actin and were therefore identical to the structures giving rise to the immunofluorescence patterns. After viewing CB-treated preparations by whole-mount TEM, we examined the cells by scanning electron microscopy (SEM). Direct SEM comparison of the filament-rich zones seen by TEM showed that these structures resulted from the formation of short lamellipodial protrusions below the site of particle binding. Electron micrographs of thin-sectioned material established that these lamellipodial protrusions were densely packed with microfilaments that were in part associated with the cytoplasmic surface of the plasma membrane. The formation of particle-associated lamellipodia did not appear to represent merely a slower rate of ingestion in the presence of CB, because they formed within minutes of particle contact with the cell membrane and were not followed by particle ingestion even after a 1-h or longer incubation. Furthermore, their formation required cellular energy. These results suggest that cytochalasin B blocks phagocytosis of large particles by affecting the distances over which any putative actomyosin-mediated forces are generated.

Cytochalasin B (CB)[1] and related drugs are well-known inhibitors of cell motile processes, including particle phagocytosis (for a review, see reference 9). Phagocytosis of large particles by a variety of mammalian cell types, including macrophages, is effectively inhibited in a rapidly reversibly manner by 10^{-6}–10^{-5} M concentrations of CB and even lower concentrations of other cytochalasins (1). The mechanism of action of the cyto-

[1] *Abbreviations used in this paper:* β-ME, β-mercaptoethanol; CB, cytochalasin B; Fl-Av, fluorescein-avidin; PBS, phosphate-buffered saline (20 mM sodium phosphate [pH 7.2]/0.13 M NaCl); Rh-Con A, rhodamine-concanavalin A; TBS, Tris-buffered saline (20 mM Tris-HCl-0.14 M NaCl [pH 8.0]); TEM, transmission electron microscopy.

THE JOURNAL OF CELL BIOLOGY · VOLUME 91 NOVEMBER 1981 373-384

chalasins in vivo remains unclear, although it is generally agreed that the drug affects the organization of the actin-containing microfilament system thought to be responsible for cell motile behavior (1, 9, 17, 32). Recent evidence obtained in vitro suggests that the drug binds to the growing ends of F-actin filaments thereby blocking further G-actin monomer addition (4, 5, 22, 23) and leading to a net reduction in the rate of filament growth. It has been suggested that this process if extended to a dynamic in vivo situation would result in a net depolymerization of cellular F-actin. This so-called treadmill model assumes that a cellular process exists for depolymerizing existing F-actin (4, 22). This model, however, is not consistent with a number of electron microscopy studies that show no drastic decrease in F-actin content in CB-treated cells as compared with controls (1, 10, 20, 29). In addition, concentrations of CB required to inhibit actin polymerization per se are generally higher than that required to block phagocytosis (4, 5, 22, 23).

Other possible mechanisms based largely on in vitro results have been advanced. Hartwig and Stossel (16) as well as Weihing (44) showed that CB inhibited the ability of cell extracts to form cross-linked actin gels at concentrations 10-fold lower than that required to block phagocytosis. Recently, Pollard and collaborators (23, 30) have provided evidence that CB may act directly on actin filaments disrupting inherent filament-filament interactions and thereby reducing the bulk polymer strength of the network and affecting the ability to propagate long-range forces. Stossel and colleagues (17, 25) have presented evidence suggesting that CB acts to disrupt network formation by acting directly on actin filaments. These authors, unlike Pollard and collaborators, present evidence that suggests that the drug causes a net shortening of filaments (but not depolymerization) that seriously weakens the strength of the gel network (17, 25). The effect of CB on the long-range strength of actin gels at physiologically effective concentrations is, in fact, consistent with several reports that indicate that the cytochalasins are ineffective in blocking phagocytosis of relatively small particles (14). Although it may be that the mechanism of ingestion of these particular particle types is fundamentally different from that operating for larger particles, it seems possible that a weaker gel network might be capable of generating enough mechanical work to allow endocytosis of sufficiently small objects.

We and others have previously found, using immunofluorescent localization techniques, that F-actin (1, 2, 9, 10, 15, 24, 29, 32, 35), myosin (29, 37), and actin-binding protein (37) appear to concentrate at particle ingestion sites in macrophages. Apparent accumulation of F-actin (1, 9, 10, 29) and myosin (29) has been reported at particle binding sites in CB-treated phagocytes. To more precisely interpret the observed increases in fluorescent staining associated with these proteins at particle binding sites, we have studied this process by a variety of morphologic techniques including correlative light and electron microscopy procedures (scanning electron microscopy, SEM; transmission electron microscopy, TEM). These studies indicate that, under conditions where CB inhibits particle ingestion, lamellipodia containing F-actin and myosin form in an energy-dependent fashion at the base of the surface-bound particle. These results suggest that the basic cellular response to particle binding to the cell membrane is not affected by the cytochalasins and further suggest that the effect of the drug is to interfere with the distances over which actomyosin-generated forces are transmitted along the cell surface.

MATERIALS AND METHODS

Preparation of Human Uterine Myosin and Anti-myosin-heavy-chain Antibodies

Human uterine smooth muscle myosin was prepared from fresh surgical specimens. Myosin was prepared from such specimens as described by Pollard et al. (31). The material was further purified by DEAE Sephadex A-50 as described by Wang (43).

Uterine myosin heavy chain was purified by preparative electrophoresis as follows: 1 mg of DEAE-purified myosin was dissolved in 0.5 ml of 4% SDS/1% β-mercaptoethanol (β-ME) and boiled for 2 min. The entire sample was applied to a 3-mm-thick slab gel consisting of a 5% acrylamide lower running gel 9 cm long and a 3% stacking gel 1 cm long. The two gel layers were prepared as described by Laemmli (21). The sample containing 10% sucrose and 0.1% bromophenol blue was applied to the stacking gel, which was prepared by omitting the toothed comb so that the sample was applied across the entire gel. The sample was electrophoresed at 20 V (constant voltage) until the tracking dye reached the end of the gel. The gel was stained with Coomassie Blue for 2 h and destained for 1 h with 10% acetic acid to a degree sufficient to allow the myosin heavy chain band to be easily seen. The band was excised with a clean razor blade. After rinsing for 1 h in 100 ml of PBS, the gel was homogenized in 10 ml of PBS with a Sorvall Omni mixer (DuPont Co., Wilmington, Del.) equipped with a microhomogenizer attachment.

1 ml of the homogenate was mixed with 1 ml of Freund's complete adjuvant (Difco Laboratories, Detroit, Mich.) and emulsified with the Omni mixer. A goat was immunized by intramuscular injections of the emulsion at multiple sites. The animal was boosted at monthly intervals three times. 10 d after the last injection, at which time serum samples showed antibodies against native myosin as judged by Ouchterlony analysis, the animal was exsanguinated, and collected serum was stored at −20°C until further use.

The antimyosin antibodies were then affinity-purified on a Sepharose 4B (4-ml packed bed) column to which 4 mg of DEAE-purified native myosin had been covalently attached as described elsewhere (29).

Extracts of human uterine tissue were prepared as described by Pollard et al. (31). Washed human platelets were prepared as described by Ginsberg et al. (13) and were essentially free of erythrocytes and leukocytes, as judged by Giemsa-stained smears of the final preparation. The cells (750 μg of cell protein) were washed twice with Tris-buffered saline (TBS) by centrifugation at 3,000 rpm for 20 min and the cell pellet was resuspended in 300 μl of 4% SDS/1% β-ME and placed on a boiling H_2O bath for 2 min. Mouse peritoneal thioglycolate-elicited macrophages were isolated as described (33), and SDS extracts were prepared as for platelets. These three tissue extracts were applied to 1.5-mm-thick 7% SDS slab gels and electrophoresed for 16 h at a constant voltage of 20 V. The gels were stained with Coomassie Blue and destained with 10% acetic acid. The gels were neutralized with phosphate-buffered saline (PBS) (pH 8.0) and stained with affinity-pure ^{125}I-labeled anti-human uterine myosin heavy chain (1 μg/ml at 1.2 μCi/μg) using a method described by Burridge (7) as modified by Wallach et al. (42). Autoradiography was performed by placing Kodak XR-1 x-ray film (Kodak, Rochester, N. Y.) over the dried gel strips in the presence of an intensifying screen for the indicated time intervals at −70°C.

The affinity-purified goat anti-human uterine myosin heavy chain antibodies used in the subsequent immunofluorescence studies were characterized by directly staining SDS PAGE gel strips with ^{125}I-labeled antibodies according to the Burridge method (7). As seen in Fig. 1 (lane *2*), the ^{125}I antibody predominantly labels a major Coomassie Blue–staining band of 200-kdaltons (lane *1*) in the crude uterine extract that comigrates with authentic myosin of the parent heavy chain. This labeling pattern is likewise seen in stained gels of SDS-solubilized whole human platelets (lane *4*) and in SDS-solubilized mouse thioglycolate-elicited mouse macrophages (lane *6*). In the latter two cell types, however, longer exposure times were required, even though comparable amounts of total cell protein were initially applied to the gel. In addition, labeling of a smaller peptide was observed in platelet extracts and may represent reaction of the antibody with proteolytic fragments of myosin H chain that are commonly seen in extracts (31). Quantitative densitometry revealed that the relative reactivity of the ^{125}I-labeled antibodies per unit of Coomassie Blue absorbance of the human platelet and mouse macrophage 200-kdalton peptides was 15 and 5%, respectively, when compared with the homologous peptide. Thus, the affinity-purified antibodies made against purified uterine myosin H chains are capable of reacting with H chains of human platelets and mouse macrophages, and are monospecific by these criteria.

Fluorescent Reagents

Biotinylated heavy meromyosin (BHMM) was prepared as described by Heggeness and Ash (18) as modified by Heggeness et al. (19). Fluorescein-avidin

(Fl-Av) was purchased from Vector Laboratories, Inc. (Burlingame, Calif.) and used without further purification. Rhodamine-labeled F(ab')2 fragments of rabbit anti-goat IgG antibodies were purchased from Cappel Laboratories, Inc. (Cochranville, Pa.).

Reagents and Chemicals

Paraformaldehyde and redistilled glutaraldehyde were obtained from Polysciences Inc. (Warrington, Pa). Formaldehyde was freshly prepared from paraformaldehyde. CB and zymosan A were obtained from Sigma Chemical (St. Louis, Mo.). Acrylamide and *bis*-acrylamide were obtained from Bio-Rad Laboratories (Richmond, Calif.). 2-D-Deoxyglucose was purchased from Calbiochem-Behring Corp. (La Jolla, Calif.).

Macrophage Isolation and Culture

Resident mouse peritoneal macrophages were prepared using BALB-C/St mice as described previously (33). The washed cells were allowed to adhere to 16-mm glass cover-slips in culture for 24 h before use. For whole-mount TEM studies (see below) 200-mesh gold grids (Pelco, Tustin, Calif.) coated with Formvar-carbon films were used in place of cover slips.

Challenge with Opsonized Zymosan Particles

Macrophages mounted either on glass cover slips or on coated gold TEM grids were pretreated with Tris-Tyrode's bovine serum albumin (BSA) medium containing the indicated concentration of drug inhibitors (if used) for 15–30 min at room temperature. Zymosan that had been pretreated with fresh human serum was added in 10 μl of buffer at a concentration of 2×10^8 particles/ml to cover slips (200 μl) or grids (20 μl) that were oriented cell side up. At various times after particle addition, excess particles were rinsed away with medium, and the cells fixed by immediate immersion in fixative. If immunofluorescent analysis was desired, the cells were fixed subsequently for 20 min with 2% paraformaldehyde/0.1 M Na-phosphate buffer (pH 7.2) and stained for actin and myosin as described below. If the cells were to be examined by TEM, Ca^{+2}-free Karnovsky's formaldehyde-glutaraldehyde fixative was substituted and, except where indicated, the grids were processed as described below.

Immunofluorescent Staining for F-actin and Myosin

Formaldehyde-fixed cells mounted on glass cover slips were double-stained for F-actin and myosin, using the technique of Heggeness et al. (19) as modified by Painter and McIntosh (29). Briefly, cover slips were treated wtih 0.1% Triton X-100 in TBS for 2 min, rinsed in BSA-TBS, and stained for 20 min with 100 μg/ml BHMM and 100 μg/ml affinity-purified goat anti-human uterine myosin heavy chain. After thorough rinsing, the cells were counterstained with Fl-Av (50 μg/ml) and rhodamine-labeled F(ab')2 fragments of rabbit anti-goat IgG.

After washing and mounting in 90% glycerol-TBS (pH 8.0), the cells were examined with a Zeiss fluorescence microscope equipped with epi-illumination and filters that allowed the selective viewing of fluorescein and rhodamine. In preliminary experiments, cells stained with either fluorochrome alone were visible only when the appropriate filter combination was in place. Micrographs were taken on Kodak Tri-X film using 30-s exposure times. Specificity controls included addition of 10 mM Na PPi to the BHMM staining step or addition of d-biotin to the Fl-Av step. Both inhibitors of their respective reagents completely blocked cell-associated fluorescein staining but not antimyosin-associated rhodamine staining. The specificity of the antimyosin reagent was assessed by preabsorption of the antibody with 10 μg of DEAE-purified human uterine myosin. No cytoplasmic-associated rhodamine staining was noted after absorption. In addition, preadsorption had no noticeable affect on BHMM/Fl-Av fluorescein staining. In addition, preimmune goat IgG did not show appreciable staining when substituted for the goat antibodies.

Electron Microscopy of Whole-cell Mounts

Macrophages were allowed to adhere to carbon-collodion-coated 200-mesh gold grids, as described above, for 24 h in HEPES-buffered minimum essential medium containing 5% fetal calf serum (Gibco Laboratories, Inc. Grand Island, N. Y.), penicillin (100 U/ml), and streptomycin (100 μg/ml). Such cells were then subjected to a variety of experimental conditions as described in the appropriate figure legends.

In electron microscopy experiments where it was desirable to examine specimens stained with BHMM/Fl-Av for comparison with immunofluorescence results, cells were fixed and stained with BHMM/Fl-Av as described above for immunofluorescence on indexed gold grids instead of cover-slips. Such specimens were then fixed with Karnovsky's fixative after the last washing step. After rinsing with 0.1 M Na cacodylate buffer (pH 7.4), the grids were incubated for 10 min at room temperature in 1% OsO_4-0.1 M Na cacodylate buffer (pH 7.4) for 10 min. After rinsing with distilled water, we stained the specimens with 0.5% uranyl acetate (pH 4.5) for 2 h and dehydrated them by passing the grids through a graded series of ethanol-H_2O solutions after rinsing them briefly with distilled H_2O. The samples were then critical point dried from Freon 13 in a Bomar model SPC-900/EX critical point dryer. All samples for direct comparison were dried together in a single run. After the specimens were examined in a Hitachi model HU-12A transmission electron microscope at 120 kV and micrographs were taken, the specimens were sputter coated with Pt-Au in a Technics West sputter-coating apparatus (Technics West, San Jose, Calif.). The same cells were examined in a Hitachi model HS-500 scanning electron microscope with a tilt stage angle of 38° and an accelerating voltage of 20 kV.

Embedding of cells in situ on cover slips in Epon and thin sectioning was carried out as described previously (29). Sections were cut in a plane perpendicular to the cover-slip surface.

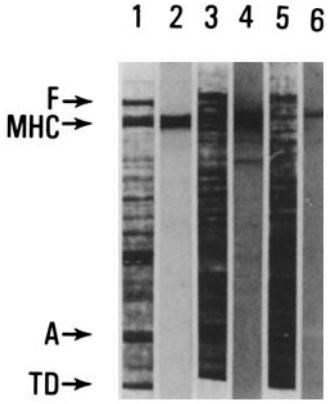

FIGURE 1 Antigenic specificity of goat anti-human uterine myosin. Tissue or cell extracts were dissolved in boiling 4% SDS/1% β-ME and applied to 7% SDS acrylamide slab gels. After staining with Coomassie Blue, each lane was cut out and labeled with ^{125}I-labeled affinity-purified goat anti-human uterine myosin using the protocol of Burridge (7) as modified by Wallach et al. (42). Lane *1*, Coomassie Blue-staining pattern obtained for human uterine extract (110 μg of protein); lane *2*, autoradiogram after 6 h of exposure; lane *3*, Coomassie Blue pattern obtained for human platelet homogenate (105 μg of cell protein); lane *4*, autoradiogram after 24 h of exposure; lane *5*, Coomassie Blue pattern for mouse thioglycolate-elicited macrophages (95 μg of protein); lane *6*, autoradiogram after 24 h. Note the major radioactive band that comigrates with myosin heavy chain (*MHC*). The electrophoretic positions of filamin (*F*), rabbit actin (*A*), and tracking dye (*TD*) are indicated by the arrows.

Drug Inhibition Protocol

Mouse resident peritoneal macrophages were allowed to adhere and spread on glass cover slips in 5% fetal calf serum/Dulbecco's minimum essential medium for 4 h before use. After rinsing with Tyrode's containing 0.25% BSA, the cells were incubated in a given drug at the indicated concentrations for 15 min before challenge with opsonized zymosan. Cells were exposed to zymosan for 30 min in the continued presence of the drug. The specimens were immediately fixed with 2% formaldehyde in 0.1 M Na phosphate buffer (pH 7.4) for 20 min. Reversal of any observed inhibitory effects was tested by rinsing the cover slip with drug-free media to remove excess drug and particles, followed by incubation in drug-free medium for 30 min.

Immunofluorescent Staining for Actin and Quantitation of Results

After fixation, cells mounted on cover slips were stained for actin using BHMM and Fl-Av as described above. To quantitate the actin response to particle binding to the cell surface, at least 200 cell-bound particles were examined at random by immunofluorescence microscopy and scored for the presence of an increased amount of F-actin-associated fluorescence associated with the particle

binding site as compared with surrounding regions of the cell cytoplasm. Several initial experiments were performed using a double-blind protocol and gave results comparable to conventionally collected data. Most of the experiments reported were not done blind, because with experience it became relatively easy for an experienced observer to distinguish drug-treated samples from controls. All results represent the mean of three or more separate experiments.

Particle Ingestion Assay

After the cells had been fixed with 2% formaldehyde/0.1 M Na phosphate buffer (pH 7.2), ingestion of zymosan was assayed as described previously (29) by counting in the microscope the number of cell-bound particles not stained and therefore not accessible to rhodamine-concanavalin A (Rh–Con A) (20 μg/ml). At least 200 particles were counted. Staining for actin was done after the cells had been treated with 0.1% Triton X-100 in TBS. Particles unstained by Rh–Con A were presumed to be within the cell. Partial staining of particles in a crescentlike pattern was also seen, indicating partial ingestion. These particles were not counted as ingested. In all cases where drugs were found to inhibit ingestion by the above criteria, no such partial or crescent forms were observed. The actin staining pattern associated with the bound particles in general was greatly enhanced in intensity as compared with surrounding cell regions and was associated with regions of the particle in direct contact with the cell surface. All data are the mean of three separate experiments. Under normal assay conditions, 30–40% of the cell-bound particles were inaccessible to Rh–Con A. If such preparations were made permeable to Rh–Con A by treatment with 0.1% Triton X-100 before staining, all observable zymosan particles were brightly stained. In addition, all particles were accessible to Rh–Con A in presence of inhibitors of phagocytosis (see Results).

RESULTS

The Effects of CB on Actin and Myosin Distributions in Macrophages Exposed to Zymosan

Macrophages pretreated with CB (10 μg/ml) showed dramatic changes in the cytoplasmic distribution of actin and myosin as revealed by immunofluorescence (Fig. 2). Actin was initially distributed in a diffuse pattern (Fig. 2*A*) with the myosin distributed in a relatively coarse punctate pattern (Fig. 2*B*), confirming our previously reported results (29). Treatment with CB for as little as 5 min at room temperature resulted in the actin and myosin patterns seen in Fig. 2*C* and *D*, respectively. The actin patterns assumed a coarse, coagulated pattern relative to that seen in untreated cells with the myosin patterns partially superimposed on the actin staining pattern. This pattern was not seen in controls even at the thinnest peripheral regions of spread cells where superposition of fluorescence was not a significant factor. Thus this pattern was not a result of CB-induced flattening of the cell caused by spreading.

When cells pretreated with CB for 15 min were exposed to zymosan for 30 min, increased staining for both actin (Fig. 3*A*) and myosin (Fig. 3*B*) was found under the bound particles in

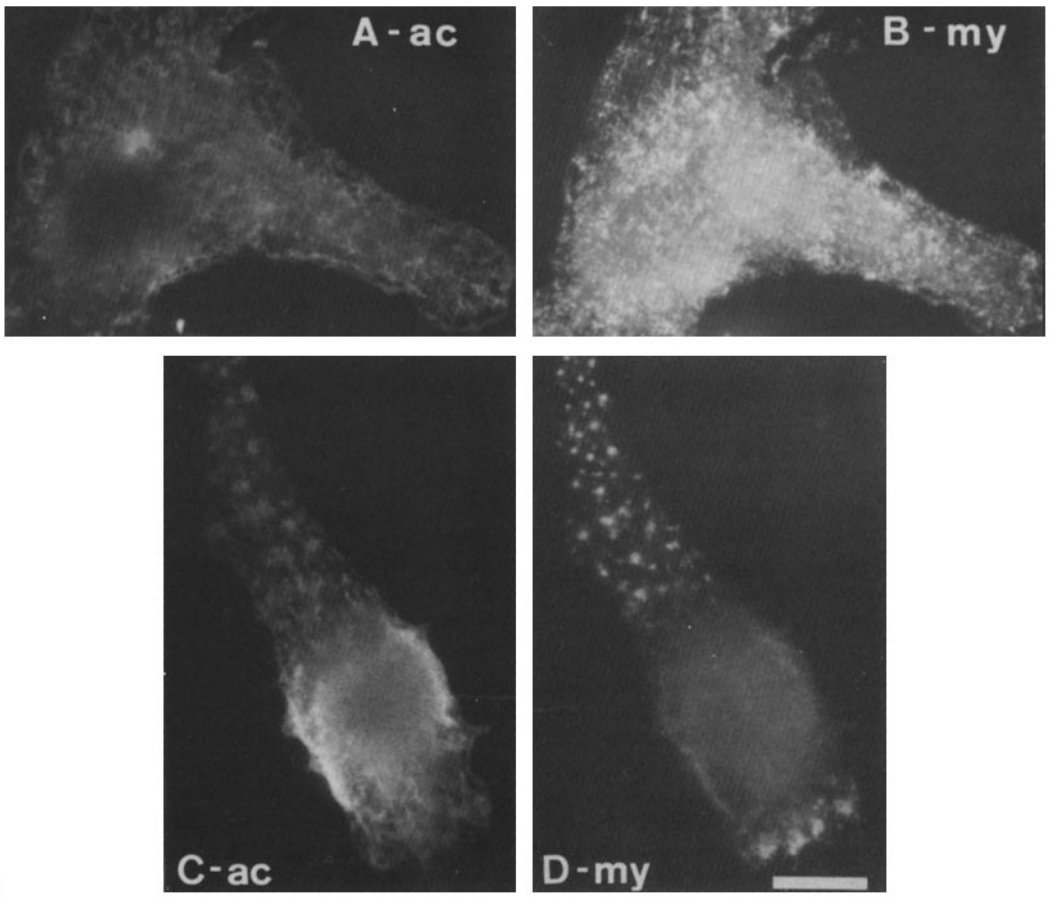

FIGURE 2 Simultaneous immunofluorescent localization of actin and myosin in resident mouse macrophages. (*A*) Actin-staining pattern (*ac*) obtained for a normal adherent mouse macrophage. (*B*) Myosin-staining pattern (*my*) in the same cell. (*C*) Actin-staining pattern (*ac*) obtained after treating the adherent cells with cytochalasin B (10 μg/ml) for 30 min at room temperature before fixation and staining as described in Materials and Methods. (*D*) Myosin (*my*) distribution in the same cell. In all cases, macrophages were allowed to adhere to cover slips for 24 h in complete medium at 37°C before the experiment. The adherent cells were then treated with Tyrode's BSA (200 μl) with (lower pair) or without (upper pair) CB for 30 min. The cells were immediately fixed with 2% paraformaldehyde and double-stained with BHMM/Fl-Av and goat antimyosin/rhodamine-labeled rabbit anti-goat F(ab')2 fragments for actin and myosin, respectively. Bar, 10 μm. × 1,250.

an oval pattern that outlined the particle periphery (arrows). The actin distribution was relatively uniform whereas the myosin distribution was patchy. Fluorescence associated with both proteins was concentrated in a plane of focus that was below the cell-bound particle. Treatment with up to 100 μg/ml CB for as long as 30 min gave similar results (not shown).

Removal of CB by washing after 15-min exposure to zymosan resulted in immunofluorescent patterns that were indistinguishable from that obtained in non-drug-treated macrophages, showing that the process was completely reversible even after the stimulus and the cell surface had been in contact for up to 30 min before drug removal (Fig. 3 *C* and *D*). It is important to note that, in the absence of the drug, the most intense staining observed was in the plane of focus of the zymosan particles. Thus, this staining is presumably associated with pseudopod extension in this case.

Quantitation of the Effect of CB on Zymosan Ingestion and the Particle-associated Actin Response

It seemed possible that the oval-shaped actin- and myosin-rich zones associated with bound zymosan in CB-treated cells could represent incomplete inhibition of ingestion attributable to a reduction in the rate of ingestion alone. To evaluate this possibility, we measured the percentage of bound particles ingested in the presence and absence of CB. This was done by determining the ability of Rh–Con A to label surface particles in fixed but intact cells. To visualize the actin distribution associated with surface and ingested particles, the cells were made permeable after Rh–Con A staining and stained with BHMM/Fl-Av. A typical result is shown in Fig. 4. In non-drug-treated controls, completely ingested zymosan is essentially unstained by Rh–Con A (Fig. 4*A*, solid arrow); this same particle showed intense staining for actin (Fig. 4*B*, solid arrow). Unexpectedly, particles that were apparently only partially ingested were seen (Fig. 4*A*, dashed arrows). Those areas of the particle surface that were inaccessible to Rh–Con A were strongly stained by BHMM/Fl-Av (Fig. 4*B*, dashed arrows).[2]

In contrast, in cells treated with CB (10 μg/ml), bound zymosan particles were completely accessible to Rh–Con A (Fig. 4*C*), and most particles had typical oval-shaped regions of actin-associated staining in a focal plane below that of the particles (Fig. 4*D*). In addition, the dimensions of the actin pattern were significantly less than the particle outline as revealed by Rh–Con A (compare Fig. 4*C* and *D*), indicating that the actin response was not attributable to substantial pseudopod formation.

Conceivably, CB could merely slow the rate of pseudopod extension around the zymosan particles. Using the Rh–Con A technique to measure ingestion, the percentage of totally ingested particles was determined in the presence and absence of CB as a function of time of exposure to particles. As documented in Table I, no particles were observed that were completely ingested even after 2 h of incubation, even though >60–80% of the bound particles had demonstrable oval-shaped actin stain in pattern associated with them. Furthermore, no partial ingestion profiles were noted. Control cells, in contrast, completely ingested up to 40–50% of bound particles in the same time period.

In our experience, the Rh–Con A technique can easily detect ingestion of at least 25% of any given individual particle. Thus, within these limits, we found no evidence to suggest that CB acted by merely slowing the rate of ingestion.

Correlative TEM and SEM of Whole Mounts of CB-treated Macrophages Exposed to Zymosan

To gain higher-resolution morphological information, we

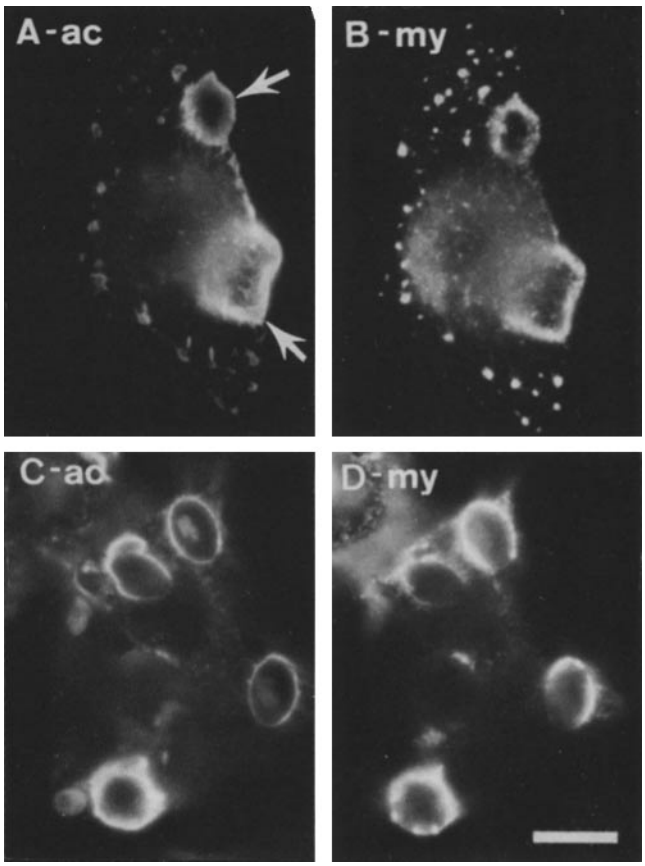

FIGURE 3 Effect of CB on actin- and myosin-staining patterns at zymosan-binding sites. Patterns of staining with (*A*) actin (*ac*) and (*B*) myosin (*my*) in the same cell, which had been pretreated with CB (10 μg/ml) for 15 min, then exposed to opsonized zymosan for 15 min before fixation and staining. Zymosan-binding sites are associated with oval-shaped zones of fluorescence seen with both fluorochromes (upper arrow). These zones are in a focal plane that lies below that of the bound particles. The larger zone of staining (lower arrow) is a site associated with a clump of zymosan particles. Note that the condensed actin- and myosin-staining patterns in those regions of the cell not associated with particles are quite similar to those seen in CB-treated cells not exposed to zymosan, as shown in Fig. 2 *C* and *D*. (*C*) Actin and (*D*) myosin distribution in a CB-treated cell that had been exposed to zymosan for 15 min in the presence of drug and then incubated in drug-free media for 15 min before fixation and staining. Unlike panels *A* and *B*, the plane of focus is through the zymosan particles and thus above the main cell body. Bar, 10 μm. × 1,125.

[2] The inability of Rh–Con A to penetrate membrane-particle interfaces is of interest with respect to the mechanism of release of lysosomal enzymes during phagocytosis. It has been suggested that release of lysosomal enzymes (some of which are comparable to Con A in molecular weight) into the medium can be explained by lysosomal fusion with phagosomes that are not yet closed to the extracellular space (45). If this is true, it is somewhat difficult to explain why the particle-membrane interface is not accessible to Rh–Con A.

performed TEM analysis of whole mounts of CB-treated macrophages on carbon-coated gold grids. Initial attempts to examine the ultrastructural elements associated with zymosan binding sites in glutaraldehyde-fixed cells (using methods described by Wolosewick and Porter [47]) were complicated by the inability of the electron beam to completely penetrate the adherent particles. In the course of our immunofluorescence localization studies, however, we noticed that ~25–30% of the actin- and myosin-rich oval-shaped zones seen in CB-treated cells exposed to zymosan were not associated with a particle. Because of their similarity in shape to that of the stained zone seen to underlie the majority of particles in such cells (and also because these structures were seen only after exposure to zymosan), we suspected that such sites represented areas where bound particles had been lost during staining.

To explore this possibility, a premarked field of such a preparation of cells was examined by phase microscopy before and after actin staining. In Fig. 5, several sites are seen (arrows) where zymosan has been lost during staining. As expected, sites at which particles were previously attached showed clear zones of actin staining.

Because particles were absent from a proportion (~25% of that associated with zymosan after staining [Table I]) of actin accumulation sites, we next examined the ultrastructural characteristics of such regions that were stained with BHMM/Fl-Av by whole-mount TEM.

Fig. 6 shows the results obtained when CB-treated and zymosan-exposed cells were fixed with formaldehyde and stained with BHMM/Fl-Av after Triton X-100 treatment. The overall morphological appearance of the transparent cell areas

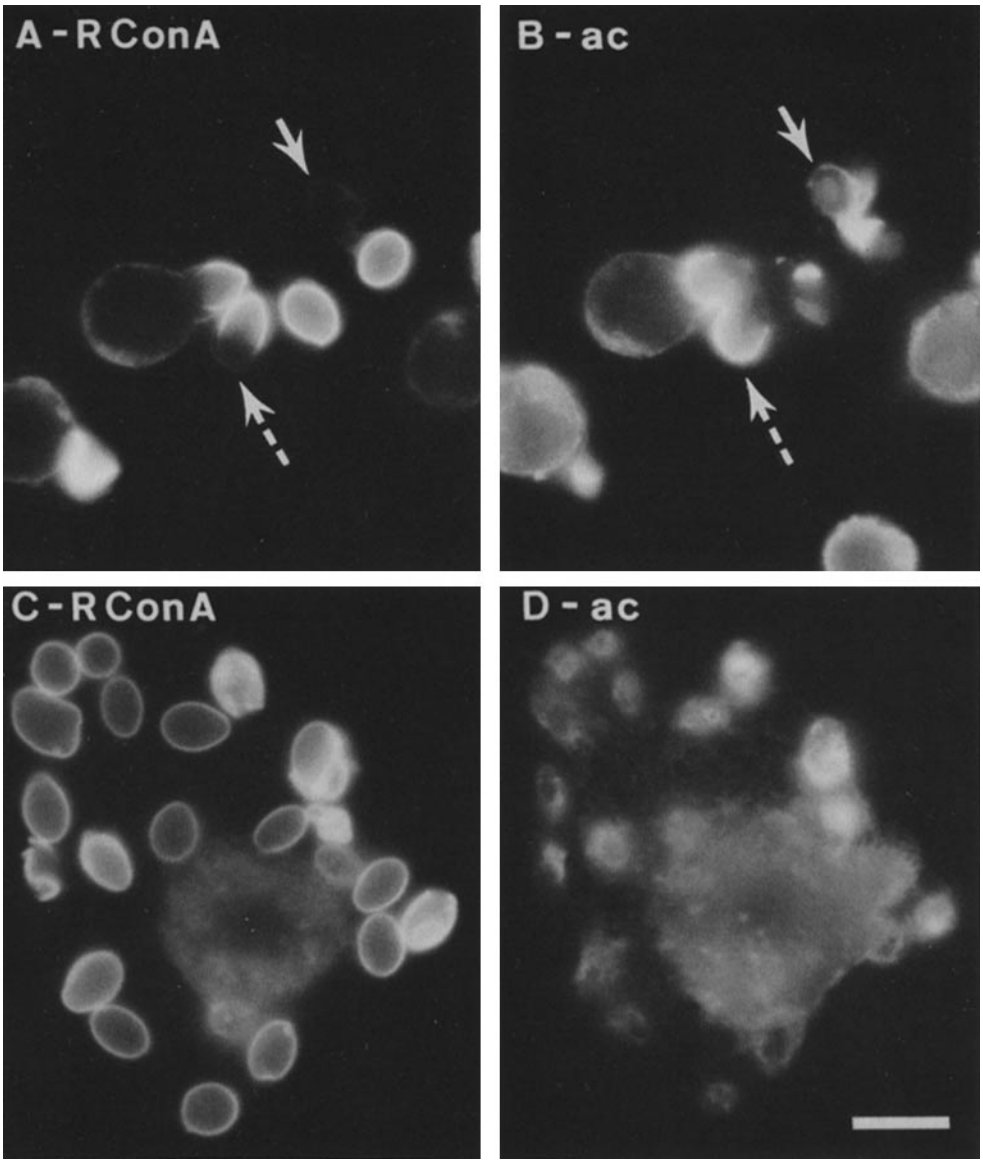

FIGURE 4 Relationship of degree of particle phagocytosis to the cytoplasmic actin distribution. After exposure to zymosan particles for 30 min in the absence (upper panels) or presence of CB (10 μg/ml, lower panels), cells were fixed and stained with Rh-Con A. After washing, the cells were made permeable with Triton X-100 and stained for actin (*A* and *C*). Note in controls (*A* and *B*) that particles in various stages of engulfment are seen ranging from complete ingestion (solid arrows) to partial ingestion (dashed arrows) and that the cytoplasmic actin-specific staining is associated with the membrane-particle interface (upper panels). No such ingestion profiles are seen in CB-treated cells (lower panels). Note that panels *A–C* are focused in the plane of the particle; *D* is focused in a plane just below the bound particles. Bar, 10 μm. × 1,250.

(Fig. 6 *A*) is reasonably similar to that seen with glutaraldehyde-fixed controls (not shown), indicating that the immunofluorescent staining procedures did not produce any gross morphological artifacts. In CB-treated cells exposed to zymosan, sites that were previously associated with particles showed a dense network of filaments that underlie former particle binding sites (Fig. 6 *C* and *D*). A similar oval-shaped zone of filamentous material is seen beneath the relatively translucent zymosan particle seen in Fig. 6 *B*, indicating that the structures seen in Fig. 6 *C* and *D* were not caused by particle detachment.

Comparison of filament diameters measured at random in these BHMM/Fl-Av preparations (Fig. 7 *A*) with those measured in formaldehyde-fixed but unstained preparations (Fig. 7 *B*) showed an increase in diameter from ~50 Å in the controls to 200 Å in the BHMM-treated samples, which was presumably the result of BHMM and Fl-Av binding to the filaments. This apparent increase in filament diameter appeared to be mediated by BHMM, because the control was treated with BSA and Fl-Av. Thus, these structures appear to correspond to the actin-containing regions revealed by immunofluorescence.

The grid matrix position of the cell shown in Fig. 6 was noted, the specimen subsequently sputter coated with Pt-Au, and the same cell as seen in Fig. 6 examined by SEM. This approach revealed, as can be seen in Fig. 8, that the dense oval-shaped zones of filaments seen in these stained cells were identical to regions where rather stubby lamellipodia (arrows) had formed, presumably as a result of particle-cell interactions. This can best be seen by direct comparison of Figs. 6 and 8. Thus, the oval-shaped actin- and myosin-associated fluorescent zones detected by immunofluorescence are identical to these lamellipodial structures and form only after interaction of zymosan with the cell surface.

TABLE I

*The Effect of CB on Particle Ingestion and Particle-associated Actin Staining**

Treatment	Incubation time	Zy/Cell	% Ingestion	% Particles with associated actin
	min			
DMSO control	15	1.2	4	85
	30	7.4	27	90
	60	8.3	45	88
	120	9.6	51	ND
CB (10 μg/ml)	15	0.8	<0.5	80
	30	5.1	<0.5	75
	120	6.2	<0.5	82

* Macrophages on cover slips were preincubated at room temperature with CB (10 μg/ml) or DMSO (0.1%) for 15 min and opsonized zymosan (*Zy*) was added (40 Zy/cell) in a total volume of 200 μl of Tyrode's BSA medium. Cover slips (in duplicate) were fixed at the indicated times with 2% formaldehyde/0.1 M Na phosphate (pH 7.4) for 20 min. After fixing, the cells were assayed under the microscope for total zymosan bound per cell, percent ingestion, and percent of particles showing a discernible increase in particle-associated actin as described in Materials and Methods. Results represent an average of three separate experiments. *ND*, not determined.

TEM of Oriented Thin Sections

To determine whether the lamellipodia-like structures seen in CB-treated cells after exposure to zymosan were artifacts arising from the immunofluorescent staining procedures employed, CB-treated cells were fixed with Karnovsky's glutaraldehyde-formaldehyde fixative after exposure to zymosan for 15 min. These cells were embedded *in situ* in Epon and thin sectioned in a plane perpendicular to the substratum.

As seen in Fig. 9, CB-treated cells clearly show zones of 70-Å microfilaments that appear to contact the cytoplasmic membrane surfaces including plasma membrane surfaces in contact with zymosan and intracellular vacuoles (arrows). These filament-rich regions were usually associated with slight protrusions of the overall cell surface that could best be described as rather stubby pseudopods. These structures on average ranged from 0.2 to 0.3 μm in length and were usually found to lie within the particle periphery. After extended incubation times of up to 2 h, the structures did not grow in length or appear to advance around the surface of the particle (not shown). Thus, the lamellipodial structures observed by SEM of immunofluorescently stained cells are demonstrable in well-fixed and thin-sectioned cells and contain microfilamentous structures.

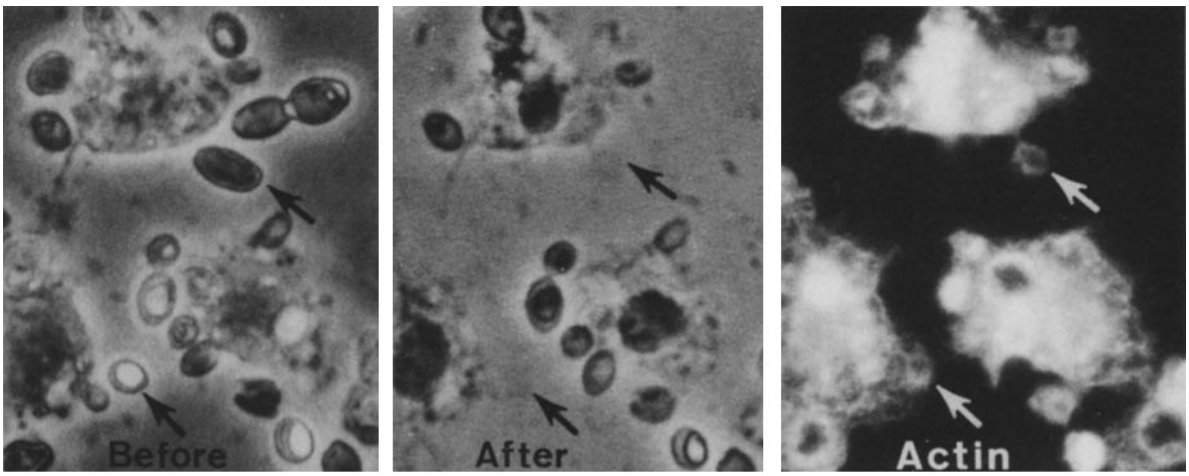

FIGURE 5 Immunofluorescent localization of F-actin at sites of particle loss in CB-treated macrophages exposed to zymosan. A predetermined and marked field of cells, which had been exposed to zymosan after CB treatment as in Fig. 3, was photographed immediately after formaldehyde fixation, using phase-contrast optics. The specimen was then stained as usual for actin as described in Materials and Methods. After relocating the same field of cells, the phase-contrast image (middle panel) and the actin-associated immunofluorescence (right panel) were photographed. As indicated by the arrows, several zymosan particles have been lost as a result of staining. As shown by the right panel, these sites show regions of actin-associated immunofluorescence that are indistinguishable from sites with associated zymosan. × 920.

Effect of Metabolic Inhibitors on Formation of Particle-associated Lamellipodial Structures in CB-treated Macrophages

Table II shows the effect of metabolic inhibitors on the formation of actin-containing lamellipodia. As assessed by immunofluorescence, 10 mM NaN_3 completely and reversibly blocked the formation of the oval-shaped actin-containing structures in CB-treated or non-CB-treated macrophages. As expected, no detectable ingestion of zymosan was noted in the presence of either CB or azide alone.

In addition, the actin-rich lamellipodial structures preformed in CB-treated cells are present even after 30 min of incubation in CB-free NaN_3 medium (Table II; line *5*). Because lamellipodia do not form in the presence of NaN_3 (Table II; line *6*), this result indicates that the lamellipodia formed in CB-treated cells after particle contact with the cell are stable structures that persist for at least 30–60 min.

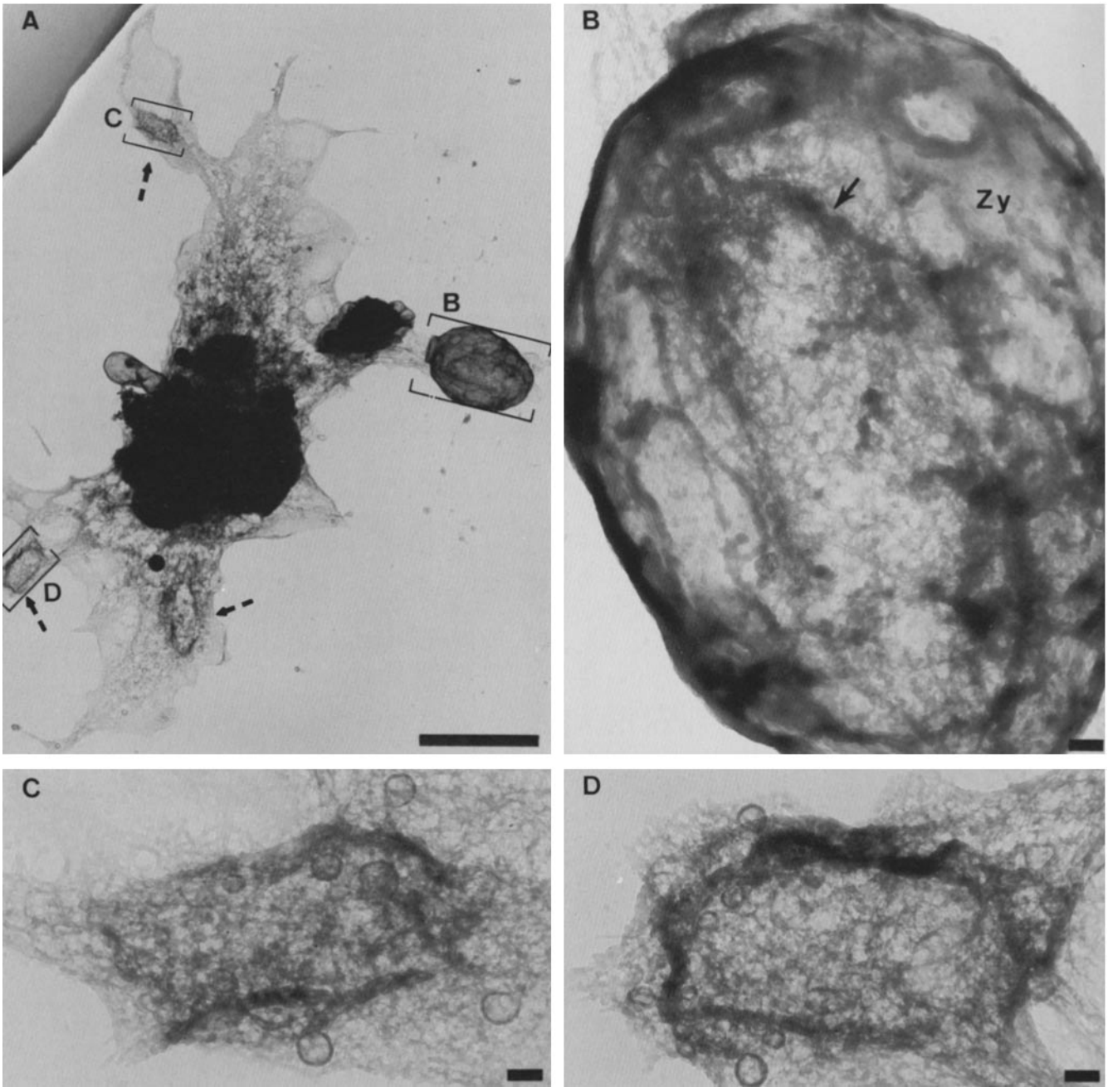

FIGURE 6 Transmission electron microscopy of CB-treated macrophages exposed to zymosan and stained for actin with BHMM/Fl-Av. (*A*) Low-magnification micrograph of a CB-treated macrophage that had been exposed to zymosan and subsequently stained for actin by use of the Heggeness and Ash technique (18). After staining, the specimens were postfixed with Karnovsky's fixative and processed as described by Wolosewick and Porter (47). This cell shows an example of a particle that was sufficiently electron transparent to show an outline of an underlying filamentous network (dashed arrows) and two sites where particles were lost during processing. These sites are shown at higher magnification in panels *B* through *D* as indicated by the bracketed areas. Note in panel *B* the filamentous zone underlying the zymosan particle (arrow). (*A*) Bar, 5 μm. × 3,600. (*B–D*) Bars, 0.2 μm. × 27,000.

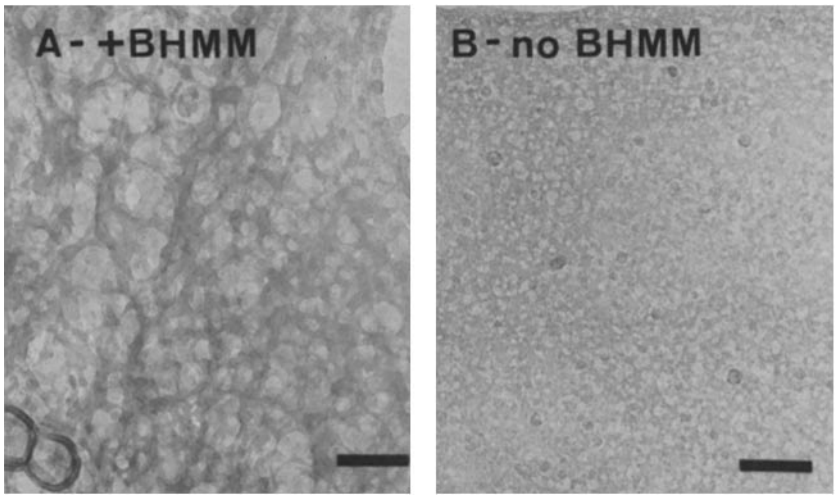

FIGURE 7 Comparison of whole-cell mounts by TEM before and after staining with BHMM/Fl-Av. (*A*) A micrograph of the BHMM/Fl-Av-stained preparation. (*B*) A sample identical in preparation to that seen in *A*, except that staining with BHMM was omitted. Accelerating voltage, 125 kV. Bars, 0.2 μm. × 48,000.

DISCUSSION

The major finding of this work is that particle binding to macrophage surfaces induces rapid and energy-dependent formation of actin- and myosin-containing lamellipodia at the particle base in the presence of concentrations of CB sufficient to block particle ingestion. The lamellipodia formed after particle contact are similar to true pseudopods formed in non-CB-treated cells in that they contain both major contractile proteins and their formation appears to require metabolic energy (Table II). However, they do not merely represent a slower rate of pseudopod advancement around the particle surface, because they form within minutes of particle contact and do not appear to advance further even after 2 h of incubation.

The Association of Actin and Myosin with Particle-induced Lamellipodial Structures

The presence of F-actin in CB-treated cells is well-documented (1, 9, 10, 29, 32). The present work is in agreement and further shows that particles capable of activating the contractile apparatus induce the accumulation of actin filaments at their sites of binding in cells pretreated with CB. The evidence that these filaments are, in fact, F-actin is based on their morphological appearance and, more significantly, their ability to bind heavy meromyosin (Figs. 3 and 7), a reagent that is specific for the filamentous form of actin but not for G-actin (27).[3]

A variety of evidence suggests that at least a fraction of the particle-associated actin appears to be associated physically with the cytoplasmic face of the membrane. For example, Fig. 9 shows 50- to 70-Å filaments that appear to make close contact with the membrane. In fact, membranes associated with 1-μm latex particles isolated in our own laboratory contain F-actin and myosin as assessed by immunofluorescent staining and by SDS PAGE. Furthermore, the amount of actin associated with these membranes per unit of membrane protein was not detectably different when normal phagosomes were compared with latex-associated membranes obtained from CB-treated cells (R. G. Painter, unpublished observations). Thus, actin filaments appear to be, in part, associated with particle membrane binding sites, both in normal and in CB-treated cells, a finding that is similar to reports about a variety of cell systems that demonstrate actin in association with the plasma membrane and isolated surface receptors (3, 8, 12, 28, 34).

Myosin is also present in lamellipodia formed at particle membrane binding sites in CB-treated cells. The presence of the two major force-generating proteins of contraction in apparently high concentrations in lamellipodial structures raises the possibility that the formation of these structures was caused by a localized actomyosin contraction. This possibility is supported by a number of facts. First, the morphologic appearance of the forming lamellipodia in relation to the shape of the particle (Figs. 6 and 8) suggests that membrane immediately adjacent to the particle contact point (not periphery) has pleated in a direction parallel to the particle perimeter. This suggests that radial forces running parallel to the cell membrane surface have pulled the adjacent membrane surface, to which the filaments are attached, toward the particle. Second, formation of the lamellipodial structures was blocked by metabolic poisons such as NaN_3, which is consistent with an actomyosin-mediated contraction.

The Relationship between Particle-induced Lamellipodium Formation and Normal Pseudopod Formation

The lamellipodial structures that formed in CB-treated cells upon particle contact resemble, in some respects, pseudopods formed in control cells. Like lamellipodia, pseudopods contain actin filaments (1, 2, 9, 15, 29, 32, 35) and myosin (29, 37) and form in response to membrane contact with appropriate particle surfaces. In addition, the metabolic requirements for the formation of both structures are similar. These pseudopodlike structures were not attributable to a reduction in the rate of particle engulfment in the presence of the drug, because they formed rapidly and did not show further growth even after 2 h of incubation. These similarities lead us to propose that *lamellipodia seen in CB-treated cells are shorter, less extensive analogues of pseudopods seen in control cells* and thus represent an abortive form of phagocytosis. A major prediction of this concept is that the ability of CB to inhibit phagocytosis would be dependent on the size and geometry of the particle. Several reports have presented data that support this prediction. Thus,

[3] This interpretation assumes that HMM binds only to F-actin and no other cellular proteins. The validity of this interpretation is supported by the fact that sodium pyrophosphate blocks the observed fluorescent patterns in areas that correspond to filament-rich zones observed in TEM.

CB did not block ingestion of *Chlamydia psittaci*, a microorganism of <0.6 μm in diameter (14). In addition, CB, while blocking complete ingestion of larger organisms such as *E. coli* K12 (10), did not prevent formation of microfilament-rich pseudopods that partially surround the surface-bound particle (24). Our own preliminary results show that ingestion of latex particles of 0.6 μm and smaller is unaffected by CB at concentrations of up to 100 μg/ml as judged by electron microscope examinations of thin sections (R. G. Painter, unpublished observations). CB has no apparent inhibitory effect on a number of endocytotic processes, including endocytosis of small bacteria (14), absorptive pinocytosis (46), and endocytosis mediated by coated pits (46). It is interesting to note that in those cases where fluid-phase pinocytosis has been reported to be inhibited by CB, uptake was mediated by vesicles 1 μm or larger (41), a result entirely in agreement with our hypothesis. Significantly, Taylor et al. (39, 40) have recently shown that fluorescein-labeled actin microinjected into cultured cells becomes localized at sites of pinocytosis and endocytosis. Frequently, lack of inhibition of endocytosis by CB has been taken to imply that there exists a mechanism entirely different from that of phagocytosis (14, 44, 34). In view of these and our own results, we support the view (9, 10, 24, 29, 35) that evidence other than lack of inhibition by CB would be required before one could conclude that a given endocytic process is not mediated by microfilaments, at least in those cases where endocytosis of structures smaller than 0.5 μm is concerned.

Implications for the Mechanism of CB Inhibition of Phagocytosis

The cytochalasins are known to have at least two possible in vitro effects on F-actin. First, the drug inhibits actin polymerization (4, 5, 17, 22, 23, 30) by blocking monomer addition at the barbed end of growing filaments (23, 30). Blocking one end of the filament would also inhibit treadmilling of actin (4, 22). Second, the drug appears to affect bulk gel strength by blocking direct filament interactions (23, 30) and/or by reducing the length of F-actin filaments (17, 25). Both effects would be expected to drastically alter the overall bulk strength of the cytoplasmic gel. The results obtained here indicate that lamellipodia form in CB-pretreated cells in response to particle

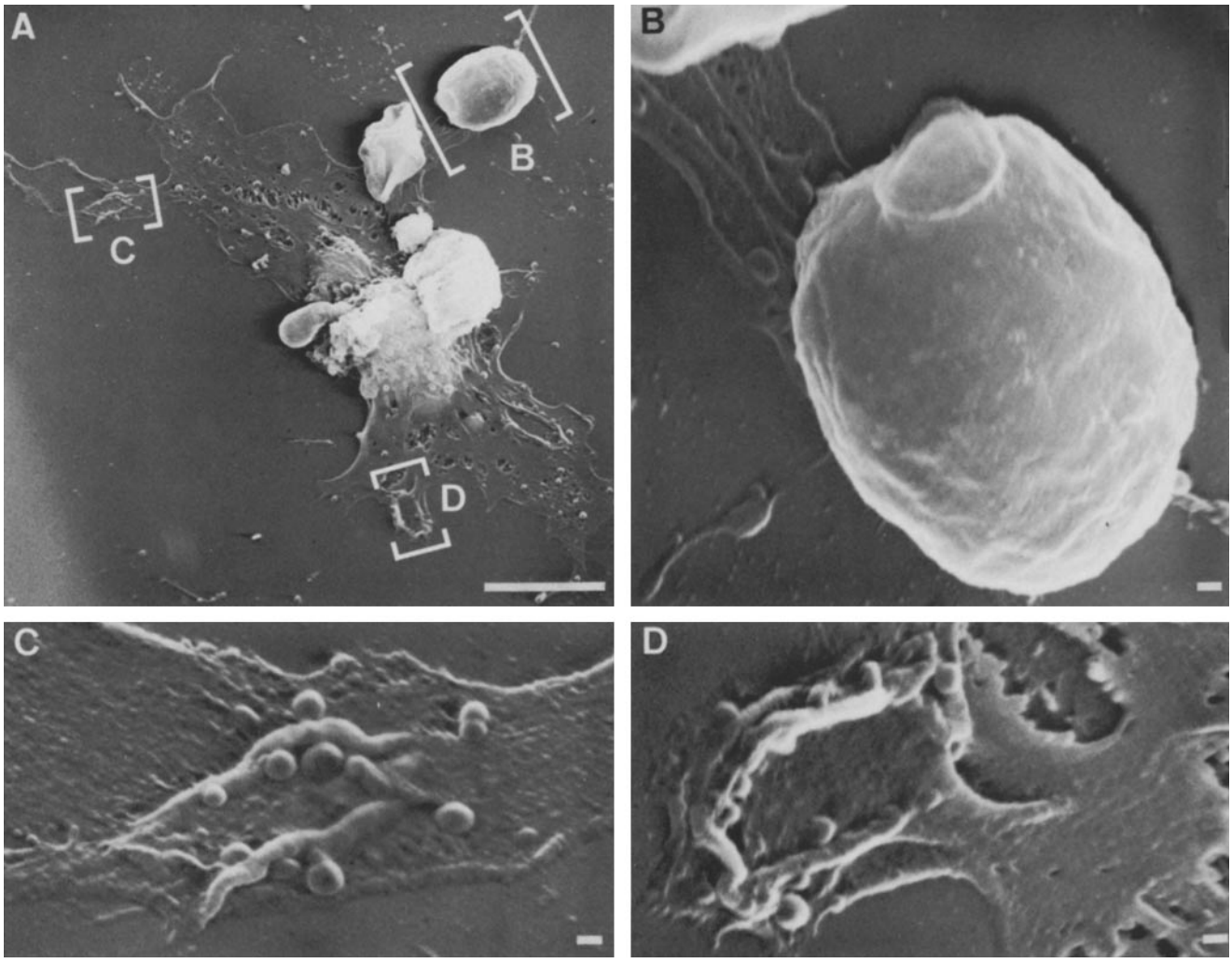

FIGURE 8 Scanning electron micrographs of the same cell as shown in Fig. 6 after sputter coating with Pt/Au. The panels labeled *A–D* correspond to identical areas visualized by transmission electron microscopy in Fig. 6. Note the lamellipodia-like outcroppings of the cell surface in panel *A* (bracketed areas labeled *C* and *D*), which are seen at higher magnification in panels *C* and *D*. These lamellipodia correspond to the filament-rich zones seen in the corresponding panels in Fig. 6. Also, note the lack of pseudopodial extensions at the edge of the zymosan particle (panel *B*). (*A*) Bar, 5 μm. × 3,300. (*B–D*) Bars, 0.2 μm. × 16,500.

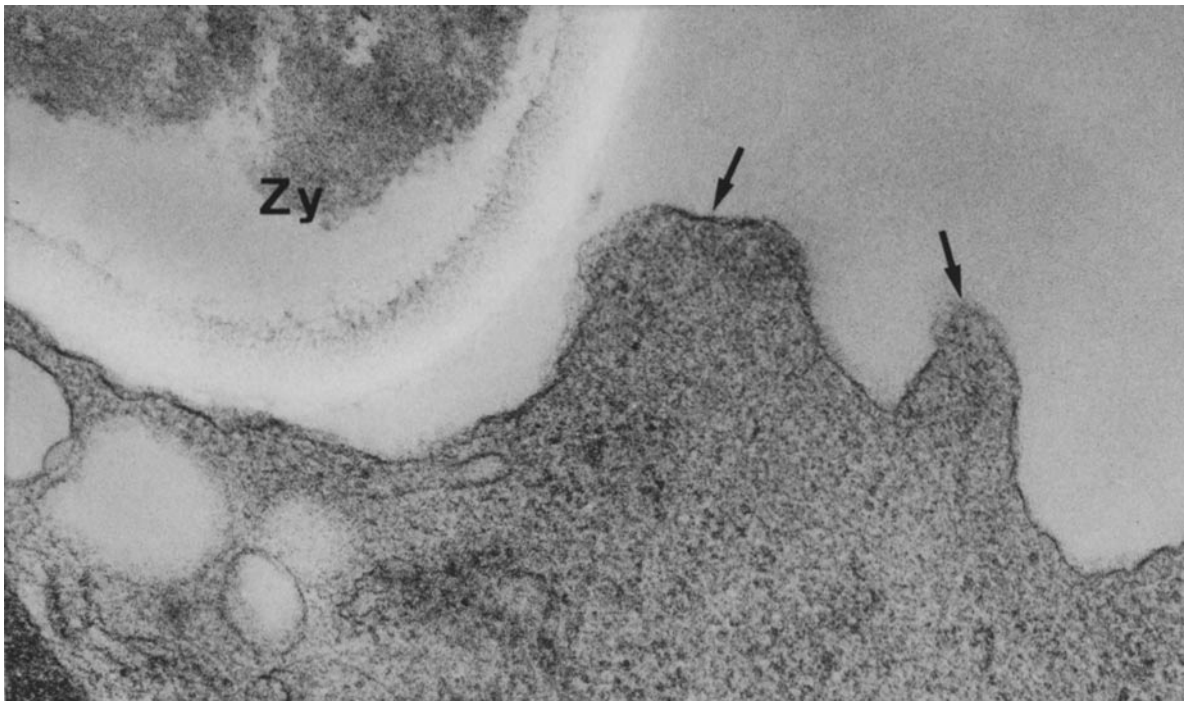

FIGURE 9 An electron micrograph of an oriented thin section of a CB-treated macrophage exposed to zymosan. Adherent CB-treated (15 min) macrophages were exposed to opsonized zymosan (*Zy*) for 15 min, fixed with Karnovsky's fixative, and embedded *in situ* in Epon. Specimens were thin sectioned perpendicular to the substratum. Note the thin filaments (50–70 Å) that appear to make contact with the cytoplasmic face of the plasma membrane (arrows) and are contained within fingerlike protrusions of the membrane surface. × 112,000.

TABLE II

Effect of Metabolic Inhibitors on the Formation of Actin-containing Lamellipodia *

Treatment 1	Treatment 2	Zy/Cell	% Ingestion	% Particles with actin-containing lamellipodia
1. DMSO	DMSO	7.2	13.5	88
2. CB, *10 μg/ml*	CB	6.2	<0.5	71
3. CB	DMSO	5.8	11.2	85
4. NaN_3, *10 mM*	NaN_3	3.8	<0.5	<0.5
5. CB	NaN_3	5.4	<0.5	61
6. NaN_3 + CB	NaN_3	2.1	<0.5	3
7. NaN_3 + CB	DMSO	3.6	9.0	87

* Macrophages on cover slips were preincubated with the drug indicated in the first column (*Treatment 1*) for 15 min at room temperature. Opsonized zymosan (*Zy*) was added at a ratio of 20 Zy/Cell and incubation continued for 30 min. After a brief rinse in drug-containing medium, cells were incubated in 200 μl of Tyrode's BSA containing the drug listed under *Treatment 2* for 30 min. The reaction was terminated by fixing the cells with 2% formaldehyde/0.1 M Na phosphate (pH 7.4) for 30 min. The percent of ingested particles was determined under the microscope by the Rh-Con A accessibility method as described in Materials and Methods. The percentage of particles with a discernible actin-staining pattern similar to that seen in Fig. 3 was taken to indicate formation of actin-containing lamellipodia. At least 200 particles per determination were scored; results represent the mean of three separate experiments.

binding. These structures apparently formed in the drug's presence and appeared to be densely packed with F-actin filaments as judged by their ability to bind HMM and by morphological criteria. It is not possible to ascertain whether these filaments were newly formed by polymerization or were recruited in the form of intact filaments from other regions of the cytoplasm. In spite of this, the data in Table I show that, once formed, lamellipodia may persist in the presence of CB for as long as 2 h. Thus, the lamellipodial actin filaments appear to be stable over a substantial period of time in CB. This suggests that CB does not act on macrophages by decreasing the number of actin filaments and that certain types of actin-containing microfilaments are not turning over rapidly in vivo. If the filaments were turning over either by treadmilling or by bulk polymerization/depolymerization, CB might be expected to alter the filament number. Both the resistance to CB and the stability of the lamellipodial filaments may arise because these filaments are attached to the plasma membrane at their barbed end, like the actin filaments in other cells (6, 11, 26, 36). Such filaments anchored to membrane sites might be resistant to the action of CB.

In view of the above considerations, our data with respect to phagocytosis are best explained by a CB effect exerted on localized gel-sol transformations, especially because the in vivo effects that we see occur in a range of drug concentrations that is similar to those required for the effects of the drug on bulk gel strength in vitro.

The authors gratefully acknowledge valuable discussions and critical review of this manuscript by Drs. Mark Ginsberg and Charles Cochrane. We thank Dr. Thomas Pollard for sharing his results with us before publication. The technical expertise of Jim Smith and Linda Kitabiashi of the Electron Microscopy department is also gratefully acknowledged. The authors thank Ms. Monica Bartlett for preparation of the manuscript.

R. G. Painter is a recipient of National Institutes of Health (NIH) Career Development Award AM-00437. This work was supported in part by U. S. Public Health Service NIH grant AI 07007.

This article is publication 2182 from the Department of Immunopathology, Scripps Clinic and Research Foundation, La Jolla, California 92037. Reprint requests should be addressed to Dr. Richard G. Painter at that address.

Received for publication 7 April 1981, and in revised form 29 June 1981.

REFERENCES

1. Axline, S. G., and E. P. Reaven. 1974. Inhibition of phagocytosis and plasma membrane mobility of the cultivated macrophage by cytochalasin B. Role of subplasmalemmal microfilaments. *J. Cell. Biol.* 62:647–659.
2. Berlin, R. D., and J. M. Oliver. 1978. Analogous ultrastructure and surface properties during capping and phagocytosis in leukocytes. *J. Cell Biol.* 77:789–804.
3. Bourguignon, L. Y. W., and S. J. Singer. 1977. Transmembrane interactions and mechanism of capping of surface receptors by their specific ligands. *Proc. Natl. Acad. Sci. U. S. A.* 74:5031–5035.
4. Brenner, S. L., and E. D. Korn. 1979. Substoichiometric concentrations of cytochalasin D inhibit actin polymerization. *J. Biol. Chem.* 254:9982–9985.
5. Brown, S. S., and J. A. Spudich. 1981. Mechanism of action of cytochalasin: evidence that it binds to actin filament ends. *J. Cell Biol.* 88:487–491.
6. Burgess, D. R., and T. E. Schroeder. 1977. Polarized bundles of actin filaments within microvilli of fertilized sea urchin eggs. *J. Cell. Biol.* 74:1032–1037.
7. Burridge, K. 1978. Direct identification of specific glycoproteins and antigens in sodium dodecylsulfate gels. *Methods Enzymol.* 50:54–64.
8. Condeelis, J. S. 1979. Isolation of Con A Caps during various stages of formation and their association with actin and myosin. *J. Cell Biol.* 80:751–58.
9. Davies, P., and A. C. Allison. 1978. Effects of cytochalasin B on endocytosis and exocytosis. *In* S. W. Tannenbaum, editor. Cytochalasins—Biochemical and Cell Biological Aspects. Elsevier/North Holland Biomedical Press, Amsterdam. 143–160.
10. Davies, P., R. I. Fox, M. Polyzonis, A. C. Allison, and A. D. Haswell. 1973. The inhibition of phagocytosis and facilitation of exocytosis in rabbit polymorphonuclear leukocytes by cytochalasin B. *Lab. Invest.* 28:16–22.
11. Edds, K. T. 1977. Microfilament bundles. I. Formation with uniform polarity. *Exp. Cell Res.* 108:452–56.
12. Flanagan, J., and G. L. E. Koch. 1978. Cross-linked surface Ig attached to actin. *Nature (Lond.)* 273:278–281.
13. Ginsberg, M. H., L. Taylor, and R. G. Painter. 1980. The mechanism of thrombin-induced platelet factor 4 secretion. *Blood.* 55:661–688.
14. Gregory, W. W., G. I. Byrne, M. Gardner, and J. W. Moulder. 1979. Cytochalasin B does not inhibit ingestion of *Chlamydia psittaci* by mouse fibroblasts (L cells) and mouse peritoneal macrophages. *Infect. Immun.* 25:463–466.
15. Griffin, F. M., Jr., and S. C. Silverstein. 1974. Segmental response of the macrophage plasma membrane to a phagocytic stimulus. *J. Exp. Med.* 139:323–336.
16. Hartwig, J. H., and T. P. Stossel. 1976. Interactions of actin, myosin and an actin binding protein of rabbit pulmonary macrophages. III. Effects of cytochalasin B. *J. Cell Biol.* 71: 295–302.
17. Hartwig, J. H., and T. P. Stossel. 1979. Cytochalasin B and the structure of actin gels. *J. Mol. Biol.* 134:539–553.
18. Heggeness, M. H., and J. F. Ash. 1977. Use of the avidin-biotin complex for the localization of actin and myosin with fluorescence microscopy. *J. Cell Biol.* 73:783–788.
19. Heggeness, M. H., K. Wang, and S. J. Singer. 1977. Intracellular distributions of mechanochemical proteins in cultured fibroblasts. *Proc. Natl. Acad. Sci. U. S. A.* 74:3883–3887.
20. Hoffstein, S., and G. Weissman. 1978. Microfilaments and microtubles in calcium ionophore-induced secretion of lysosomal enzymes from human polymorphonuclear leukocytes. *J. Cell Biol.* 78:769–781.
21. Laemmli, U. K. 1970. Cleavage of structural proteins during assembly of the head of bacteriophage T4. *Nature* 227:680–685.
22. Lin, D. C., K. D. Tobin, M. Grumet, and S. Lin. 1980. Cytochalasins inhibit nuclei-induced actin polymerization by blocking filament elongation. *J. Cell Biol.* 84:455–60.
23. MacLean-Fletcher, S. and T. D. Pollard. 1980. Mechanism of action of cytochalasin B on actin. *Cell* 20:329–41.
24. Malawista, S. E., J. B. L. Gee, and K. G. Bensch. 1971. Cytochalasin B reversibly inhibits phagocytosis: functional, metabolic and ultrastructural effects in human blood leukocytes and rabbit alveolar macrophages. *Yale J. Biol. Med.* 44:286–300.
25. Maruyama, K., J. H. Hartwig, and T. P. Stossel. 1980. Cytochalasin B and the structure of actin gels. II. Further evidence for the splitting of F-actin by cytochalasin B. *Biochim. Biophys. Acta.* 626:494–500.
26. Mooseker, M. S., and L. G. Tilney. 1975. Organization of actin filament-membrane complex. Filament polarity and membrane attachment in the microvilli of intestinal epithelial cells. *J. Cell Biol.* 67:725–743.
27. Offer, G., H. Baker, and L. Baker. 1972. Interaction of monomeric and polymeric actin with myosin subfragment 1. *J. Mol. Biol.* 66:435–444.
28. Oliver, J. M., R. Lalchandani, and E. L. Becker. 1977. Actin redistribution during concanavalin A cap formation in rabbit neutrophils. *J. Reticuloendothel. Soc.* 21:359–364.
29. Painter, R. G., and A. T. McIntosh. 1979. The regional association of actin and myosin with sites of particle phagocytosis. *J. Supramol. Struct.* 12:369–384.
30. Pollard, T. D., and M. S. Mooseker. 1981. Direct measurement of actin polymerization rates constants by electron microscopy of actin filaments nucleated by isolated microvillus cores. *J. Cell Biol.* 88:654–659.
31. Pollard, T. D., S. M. Thomas, and R. Niederman. 1974. Human platelet myosin. I. Purification by a rapid method applicable to other non-muscle cells. *Anal. Biochem.* 60: 258–266.
32. Reaven, R. P., and S. G. Axline. 1973. Subplasmalemmal microfilaments and microtubules in resting and phagocytosing macrophages. *J. Cell Biol.* 59:12–27.
33. Russell, S. W., W. F. Doe, R. G. Hoskins, and C. G. Cochrane. 1976. Inflammatory cells in solid murine neoplasms. I. Tumor disaggregation and identification of constituent inflammatory cells. *Int. J. Cancer.* 18:322–330.
34. Schreiner, G. F., K. Fujiwara, T. D. Pollard, and E. R. Unanue. 1977. Redistribution of myosin accompanying capping of surface Ig. *J. Exp. Med.* 145:1393–1398.
35. Silverstein, S. C., R. M. Steinman, and Z. A. Cohn. 1977. Endocytosis. *Annu. Rev. Biochem.* 46:669–722.
36. Small, J. V., G. Isenberg, and J. E. Celis. 1978. Polarity of actin at the leading edge of cultured cells. *Nature (Lond.)* 272:638–639.
37. Stendahl, O. I., J. H. Hartwig, E. A. Brotschi, and T. P. Stossel. 1980. Distribution of actin-binding protein and myosin in macrophages during spreading and phagocytosis. *J. Cell Biol.* 84:215–224.
38. Taylor, D. L., J. B. Hellewell, H. W. Virgin, and J. Heiple. 1979. The solation-contraction hypothesis of cell movements. *In* cell motility: molecules and organization. S. Hatano, H. Ishikawa, and H. Sato, editors. University Park Press, Baltimore. 363–378.
39. Taylor, D. L., and Y. Wang. 1978. Molecular cytochemistry: Incorporation of fluorescently labeled actin into living cells. *Proc. Natl. Acad. Sci. U. S. A.* 75:857–861.
40. Taylor, D. L., Y. Wang, and J. M. Heiple. 1980. Contractile basis of ameboid movement. VII. The distribution of fluorescently labeled actin in living amebas. *J. Cell Biol.* 86:590–598.
41. Wagner, R., M. Rosenberg, and R. Estensen. 1971. Endocytosis in Chang liver cells: quantitation by sucrose ^{3}H uptake and inhibition by cytochalasin B. *J. Cell Biol.* 50:804–817.
42. Wallach, D. P., J. A. Davies, and I. Pastan. 1978. Purification of mammalian filamin. Similarity to high molecular weight binding protein in macrophages, platelets fibroblasts and other tissues. *J. Biol. Chem.* 253:3328–3335.
43. Wang, K. 1977. Filamin, a new high molecular weight protein found in smooth muscle and non-muscle cells. Purification and properties of chicken gizzard filamin. *Biochemistry.* 16:1857–1865.
44. Weihing, R. R. 1976. Cytochalasin B inhibits actin-related gelation of HeLa cell extracts. *J. Cell Biol.* 71:303–307.
45. Weissmann, G., R. B. Zurier, P. J. Spieler, and I. M. Goldstein. 1971. Mechanisms of lysosomal enzyme release from leukocytes exposed to immune complexes and other particles. *J. Exp. Med.* 134:149S–165S.
46. Wills, E. J., P. Davies, A. C. Allison, and A. D. Haswell. 1972. Cytochalasin B fails to inhibit pinocytosis by macrophages. *Nat. New Biol.* 240:58–60.
47. Wolosewick, J. J., and K. R. Porter. 1979. Microtrabecular lattice of cytoplasmic ground substance: artifact or reality. *J. Cell Biol.* 82:114–139.